CFRP Reinforcement and Repair of Steel Pipe Elbows Subjected to Severe Cyclic Loading

CFRP REINFORCEMENT AND REPAIR OF STEEL PIPE ELBOWS SUBJECTED TO SEVERE CYCLIC LOADING[a]

Ioannis Skarakis[1], Giannoula Chatzopoulou[2], Spyros A. Karamanos[2,3], Nicholas G. Tsouvalis[1] and Aglaia E. Pournara[2]

[1] *School of Naval Architecture and Marine Engineering, National Technical University of Athens, Greece.*

[2] *Department of Mechanical Engineering, University of Thessaly, Volos, Greece.*

[3] *Institute of Infrastructure and Environment, School of Engineering, The University of Edinburgh, Scotland, UK.*

ABSTRACT

In order to ensure safe operation and structural integrity of pipelines and piping systems subjected to extreme loading conditions, it is often necessary to strengthen critical pipe components. One method to strengthen pipe components is the use of composite materials. The present study is aimed at investigating the mechanical response of pipe elbows, wrapped with Carbon Fiber Reinforced Plastic (CFRP) material, and subjected to severe cyclic loading that leads to low-cycle fatigue. In the first part of the paper, a set of low-cyclic fatigue experiments on reinforced and non-reinforced pipe bend specimens are described focusing on the effects of CFRP reinforcement on the number of cycles to failure. The experimental work is supported by finite element analysis presented in the second part of the paper, in an attempt to elucidate the failure mechanism. For describing the material nonlinearities of the steel pipe, an efficient cyclic-plasticity material model is employed, capable of describing both the initial yield plateau of the stress-strain curve and the Bauschinger effect characterizing reverse plastic loading conditions.

[a] An early version of this paper has been presented in ASME PVP Conference 2016, Vancouver, BC, Canada; Paper PVP2016-63853: *Numerical simulation of CFRP reinforced steel pipe elbows subjected to cyclic loading.*

The results from the numerical models are compared with the experimental data, showing an overall good comparison. Furthermore, a parametric numerical analysis is conducted to examine the effect of internal pressure on the structural behavior of non-reinforced and reinforced elbows, subjected to severe cyclic loading.

1 INTRODUCTION

Pipe bends or "elbows" constitute critical components of transmission pipelines and piping systems. Under extreme cyclic-loading conditions (e.g. earthquakes, shut-down conditions), the mechanical response of pipe bends is quite unique, characterized by a biaxial state of stress and strain, which may cause failure of the piping component in low-cycle fatigue or ratcheting, associated with pipe wall rupture and loss of containment. Numerous studies have been published on the mechanical response of pipe elbows, to understand and quantify this unique mechanical behavior. Sobel and Newman [1] investigated the in-plane bending buckling of a pipe elbow comparing experimental results reported in [2] and simplified finite element analysis. Gresnigt and Van Foeken [3] investigated experimentally the strength and deformation capacity of pipe bends in pipelines. In that paper, improved analytical models for elastic and plastic design were also presented, and the results were compared with experimental and numerical calculations. Chattopadhyay *et al.* [4] proposed empirical equations to evaluate the collapse moment of elbows under internal pressure and in plane bending. Experimental work on ratcheting of pressurized pipe elbows has been conducted by Yahiaoui *et al.* [5]; short-radius welding bends were tested under conditions of constant internal pressure and in-plane resonant dynamic moments that simulated seismic excitations. Fujiwaka *et al.* [6] performed pipe component tests to clarify the fatigue life under various severe cyclic loading conditions. In a series of papers, Karamanos *et al.* [7], [8] reported several studies towards assessing the mechanical response and mode failures of pipe elbows under in-plane and out-of-plane bending, considering both monotonic and cyclic load cases. This work has been extended on the bending behavior of externally pressurized induction bends, used in offshore pipe applications as reported by Pappa *et al.* [9]. Takakashi *et*

al. [10] performed in plane-bending low-cycle fatigue tests on pipe elbows specimens with local wall thinning, due to metal loss from erosion corrosion. More recently, the low-cycle fatigue of pipe elbows, subjected to severe cyclic loading, has been investigated experimentally and numerically by Varelis *et al.* [11], [12]. The recent paper by Karamanos [13] offers an overview of pipe elbow mechanical behavior under severe loading conditions.

Wrapping of pipe elbows using Glass Fiber Reinforced Plastic (GFRP) or Carbon Fiber Reinforced Plastic (CFRP) constitutes a promising method for preventing elbow failure. Based on available experimental, analytical and numerical results described in the previous paragraph, the elbow ovalization mechanism constitutes the major cause of pipe wall cracking under cyclic loading. In the case of strong repeated loading, it is expected that wrapping would reduce ovalization of the pipe bend, resulting in lower local strains, thus increasing its fatigue life. Previous research on this subject has been directed towards the reinforcement of large diameter pipelines and pipe elbows, with the purpose of improving their structural integrity against pressure containment. Relevant studies have been reported on where the use of composite materials to repair and strengthen pressurized transmission pipelines against corrosion, dents, wrinkle bends and other pipe wall anomalies and in other hand to reinforce large diameter pipe elbow subjected to extreme bending loading [14],[15],[16],[17]. A more recent study focused on the repair of offshore pipe risers using composite materials [18], considering three conditions of corroded pipe riser. In subsequent studies, Mokhtari *et al.* [19], [20] investigate the influence of using CFRP wrap on buried pipelines against permanent ground deformation and subsurface explosion. Furthermore, Alton *et al.* [21] investigate the use of CFRP patch as reinforcement to a storage tank during a seismic event, in an effort to mitigate the formation of elephant foot buckling.

The present study examines reinforcement and structural rehabilitation of pipe elbows with composite materials for the case of severe structural bending loading. It examines the question whether the CFRP wrap material is capable of improving the structural performance of a pipe elbow, subjected to cyclic loading, and increasing its fatigue life by reducing the effects of cross-sectional ovalization, which constitutes the main failure mechanism. The study combines

experimental testing with numerical simulations, with the purposes of (a) describing accurately the mechanical response of elbows reinforced with CFRP wrapping and (b) comparing their behavior with non-reinforced elbows in an attempt to quantify the effects of CFRP reinforcement. Experiments on seven (7) carbon steel elbows are performed [four (4) non-reinforced and three (3) reinforced], under severe cyclic-loading conditions, and their mechanical strength is determined in terms of low-cycle fatigue resistance against pipe wall through-thickness fracture. Prior to elbow experiments, small-scale coupon tests have been performed to determine the mechanical properties of the elbow steel material, under both monotonic and cyclic loading conditions. Numerical finite element models have also been developed, based on shell element discretization, whereas a von Mises cyclic-plasticity constitutive model is developed, and implemented using a material-user subroutine to describe nonlinear material behavior. The constitutive model is based on the nonlinear kinematic hardening rule, appropriately enhanced to account for the initial yield plateau and the Bauschinger effect. The results obtained from the numerical models are compared with the experimental results, towards numerical model validation. Finally, some important conclusions on the efficiency of CFRP wrapping reinforcement on pipe elbows are presented at the end of the paper.

2 EXPERIMENTAL PROCEDURE

2.1 Specimens and set up for cyclic loading

In the framework of the present study, seven tests were conducted on 4-inch (114.3 mm) diameter long-radius induction bends (elbows). The elbow specimens are depicted in Fig. 1. The elbow nominal diameter and thickness were are equal to D=114.3 mm and t=3.6 mm respectively, with R/D ratio value equal to 1.5 (long-radius bends). The elbow was connected to two straight pipes with the same nominal diameter and thickness, while each straight pipe had a length equal to 400 mm. The material of the elbow specimens was steel grade EN P235.

Fig. 1: Steel elbow specimens.

A unidirectional carbon/epoxy composite system was used as reinforcement in the form of 50-mm-wide strips, which were helically wrapped around the pipe, with their wrap direction almost aligned in hoop direction of the pipe (Fig. 2). The composite system consisted of the UD Tyfo SCH-11UP fabric, weighing 400 g/m^2 and Tyfo-S epoxy system. These materials were provided from FYFE. The Young's modulus values of the CFRP reinforcement were E_1=85 GPa in hoop direction (direction of fibers) and E_2=6 GPa in axial direction of the pipe. The thickness of each composite layer was equal to ½ mm. The composite system was applied around the pipe elbow with the hand lay-up method with a total of five layers of CFRP wrap for each specimen. During wrapping of the CFRP layers on the specimen, a variation of the composite material thickness along the circumferential direction of the pipe elbow was observed, due to the different level of overlapping strips.

Fig. 2: Implementation of the CFRP patch on the pipe elbow.

The experiments took place at the facilities of the Shipbuilding Technology Laboratory at the National Technical University of Athens. The experimental set-up for the cyclic tests is presented in Fig. 3 (a) and (b) and consisted of one hydraulic actuator connected with hinge at the top of the elbow specimen, whereas the bottom support was also hinged. The actuator imposed displacement at the upper end of the elbow, while the lower end did not move. Each pipe elbow was capped using two flanged plates, welded at the end sections. Proper alignment between the two supports had been applied, alleviating possible out-of-plane deformation. Strain gauges were attached to the specimens to monitor local strain evolution, not only on the elbows but also on the straight pipe parts as shown in Fig. 3 (c). It should be noted that the strain gauges were located on the outer surface of the specimens. In the case of reinforced elbows, they were attached directly onto the outer surface of CFRP wrapping, and did not provide reliable strain measurements. Moreover, LVDT measurements were used at both intrados and extrados of the elbow Fig. 3 (c), in an attempt to measure the change of pipe diameter during the load cycles.

Table 1: Applied displacement range and number of cycles until failure.

Specimens	Type	ΔL(mm)	N_f
1	NR	± 20	301
2	R		1086
3(a)	NR	± 25	201
3(b)	NR		206
4	R		528
5	NR	± 30	120
6	R		238

Before testing, each specimen had been filled with water via appropriate nozzles located at the top and bottom of the specimen. A pressure gauge had been fitted at the top nozzle of the specimen, to measure the initial internal pressure and the variation of this pressure during the

opening and closing phases of the test. The initial water pressure inside the specimen had been measured equal to approximately 4 bar. This very low pressure level (less than 3% of the yield pressure ($p_Y = 2\sigma_Y t/D$)) had negligible effect on the mechanical behavior of the pipe elbow. However, it was necessary for the purpose of identifying the development of through thickness crack and the corresponding loss of containment. In Table 1, the applied displacement range ΔL and the number of cycles to failure N_f for each specimen are presented. In that table, "NR" denotes a non-reinforced specimen, while "R" refers to a reinforced specimen.

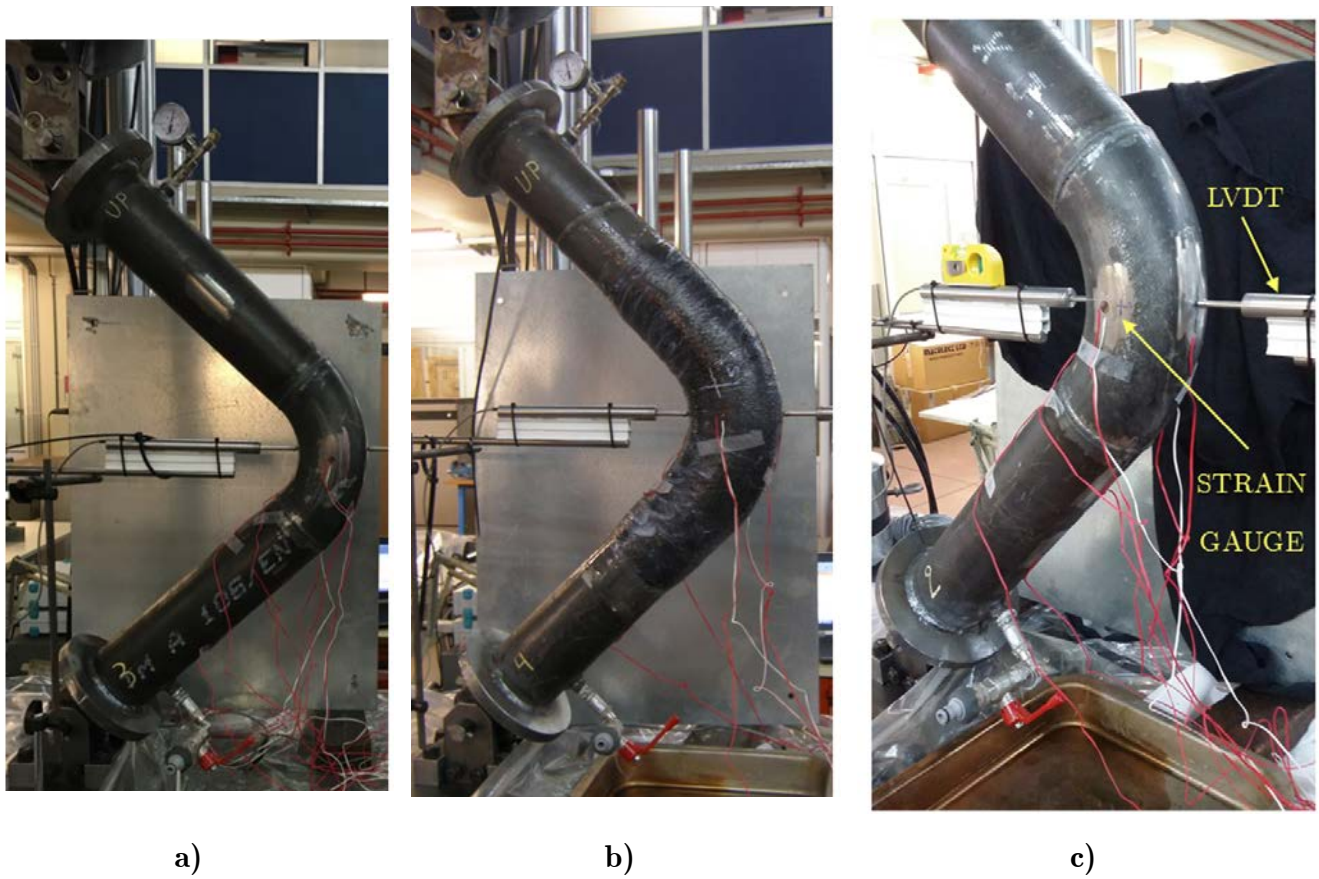

a) **b)** **c)**

Fig. 3: Experimental set-up for a) non-reinforced elbow and b) reinforced pipe elbow; c) LVDT and strain gauge locations.

2.2 Experimental results for cyclic loading

The pipe elbow specimens had been subjected to low cyclic in-plane bending through the application of cyclic end-displacement on the moving hinge at the upper end in vertical direction, keeping the lower hinge constant. The first two specimens, namely 1 and 2, were subjected to a displacement range of ±20mm, specimens 3(a), 3(b) and 4 were subjected to a displacement range of ±25mm and a displacement range of ±30mm was applied to specimens 5 and 6. Note that test 3(b) is a repeat of test 3(a). The criterion of failure was "loss of containment", associated with through-thickness fracture as discussed in the previous paragraph.

Fracture of the non-reinforced specimens occurred at the crown area due to excessive cyclic strain in the hoop direction, which is in accordance with previous publications [11], [12]. Fig. 4 (a) depicts the failure mode of the specimen after the test, in the format through-thickness crack failure of the non-reinforced specimen, associated with immediate loss of containment as shown in Fig. 4 (b). Because of internal pressure, the water sprayed out suddenly when the crack developed fully across the pipe wall thickness, despite the low-level of pressure. In the reinforced specimens, several circumferential cracks occurred at the CFRP wrap reinforcement, very soon after the start of the test. However, "loss of containment" was observed quite later at the intrados area of the composite material, at the location where the largest crack developed (Fig. 5 (a), (b)). It is particularly interesting to notice that the failure mode shown in Fig. 4 is identical for all non-reinforced specimens, while the failure mode of Fig. 5 occurred in all reinforced specimens.

Upon completion of each test on reinforced elbows, a cutting machine was used to cut the pipe elbows transversely at several locations in order to inspect the cracked area of the steel pipe. It was observed that the failure crack initiated at the steel wall thickness from the inside surface, located at the vicinity of girth welds, i.e. the area where the straight pipe was connected to the elbow as shown in Fig. 6. The detection of failure was made with the use of liquid penetrant inspection (LPI) of the failed specimens. Moreover, de-bonding of CFRP wrap had been identified between the steel pipe elbow and the CFRP reinforcement, close to the intrados area (Fig. 7).

a) **b)**

Fig. 4: a) Crack configuration at crown area in non-reinforced pipe elbow specimens; b) Loss of containment because of through-thickness crack development in non-reinforced specimen 5.

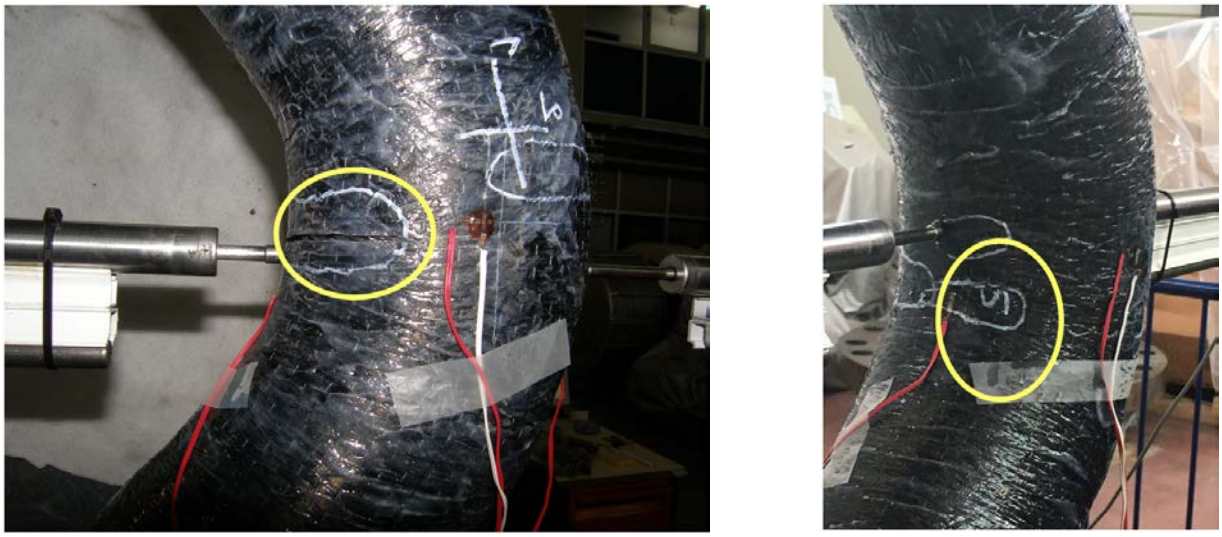

a) **b)**

Fig. 5: a) Crack failure of CFRP reinforced specimen at the elbow intrados; b) Loss of containment in reinforced pipe elbow specimen.

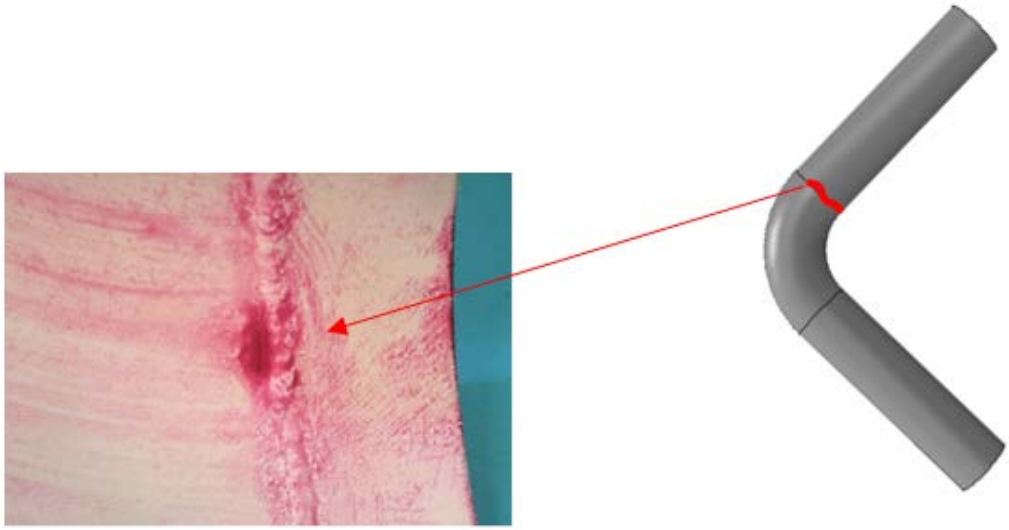

Fig. 6: Fatigue crack at the vicinity of girth weld between the elbow and the pipe, in reinforced pipe elbow-specimen No. 6.

Fig. 8 depicts the experimental force-displacement response for a few initial loading cycles for both reinforced and non-reinforced specimens, for the 3 amplitudes of applied displacement. It is worth mentioning that the CFRP reinforcement increased significantly the reaction force of the pipe elbow at the loading frame, due to the increase of stiffness provided by the CFRP wrapping.

Furthermore, the effect of CFRP wrapping on the change of pipe diameter has been examined. For each displacement range, the change of elbow diameter had been recorded by means of LVDTs for both reinforced and non-reinforced elbows. Fig. 9 depicts schematically the experimental arrangement with the LVDTs, oriented in the lateral direction. It should be noted though that, due to the set-up limitations, LVDTs were located at a specific height, so that the measurements did not refer to a specific cross section; the middle section of the elbow moved up and down with respect to the LVDT height, resulting in a certain error on the value of cross-sectional distortion under cyclic loading. In the following, the term "ovalization" it is used to refer to the change of the diameter in y direction as shown in Fig. 9. Nevertheless, despite the fact that the LVDT measurements did not represent exactly the ovalization of the middle elbow section, these measurements clearly show that cross-sectional distortion (ovalization) of the elbows reinforced with CFRP is smaller than the ovalization of the non-reinforced elbows. Table 2 presents the reduction of elbow diameter due to CFRP in comparison to non-reinforced for all

the number of cycles. The ovalization values are defined as $\Delta D/D$, where ΔD is the change of diameter in the plane of bending and D is the initial value of the diameter. For higher values of imposed displacement, numerous circumferential cracks occurred at the CFRP reinforcement right from the start of the test, and as a result, the contribution of CFRP on the reduction of cross-sectional distortion decreased in the subsequent cycles.

Fig. 7: De-bonding of the CFRP from the pipe elbow surface.

Table 2: Decrease of pipe diameter due to the presence of CFRP patch reinforcement (experimental and numerical results).

Displacement range ΔL[mm]	Percentage reduction of ovalization
± 20	31.5%
± 25	28.9%
± 30	14.3%

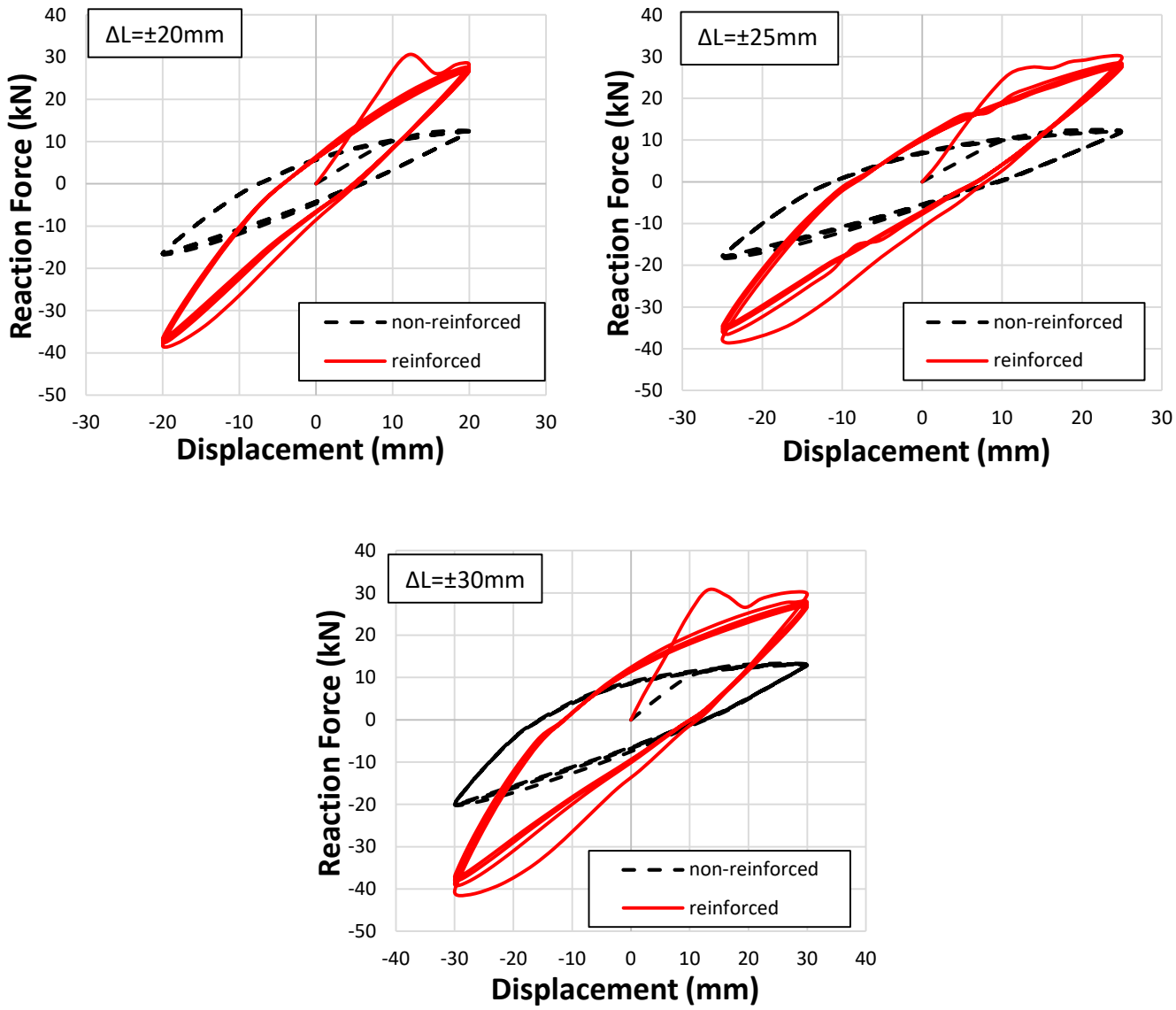

Fig. 8: Force (kN) versus displacement (mm) for ΔL equal to ±20mm, ±25mm, and ±30mm; experimental results.

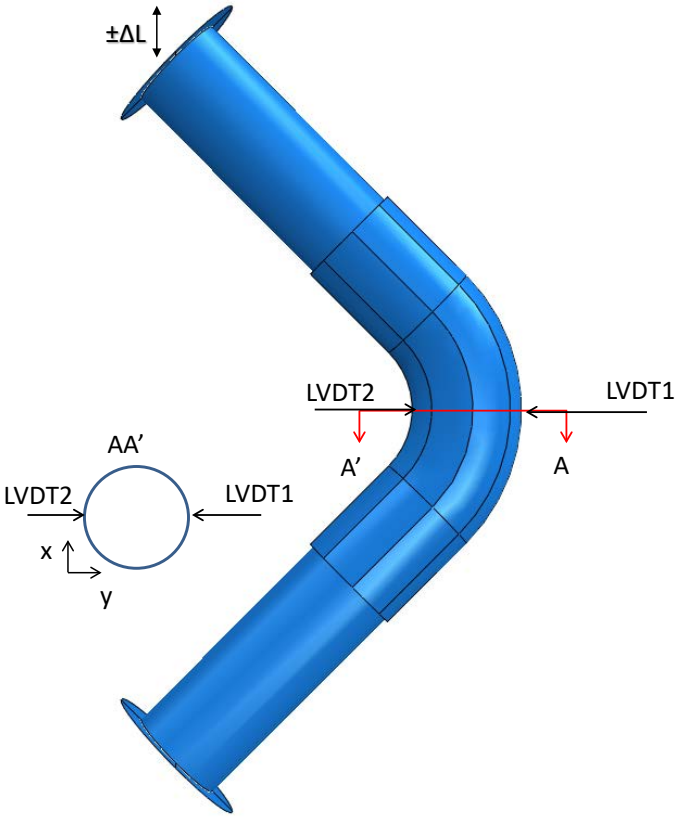

Fig. 9: Set-up of LVDTs

Furthermore, experimental measurements of hoop strains obtained from the non-reinforced elbows are depicted in Fig. 10, showing that the strain range at the elbow flank, which is the critical elbow location, fluctuated from 1.5% to 2.5% for the values of applied displacement range considered. As the applied displacement range ΔL increases, the strain range at the critical location also increases, resulting in a decrease fatigue life, as shown in Table 1.

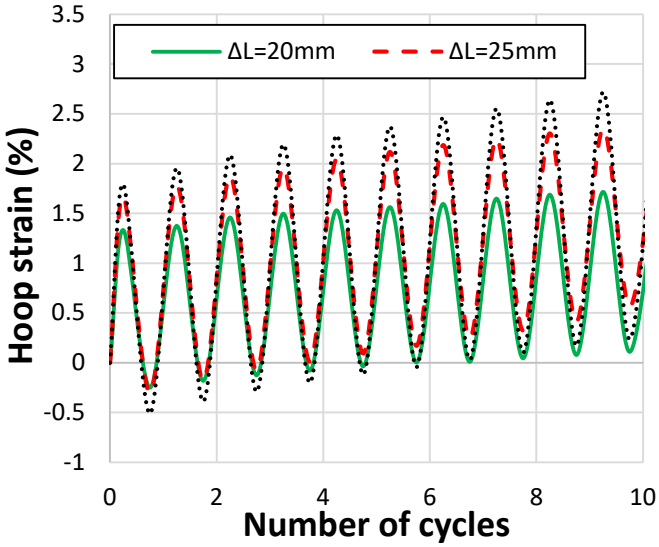

Fig. 10: Hoop strains evolution for different displacement ranges.

2.3 Pressure tests on repaired specimens

Following the cyclic loading testing procedure described in the previous section, the four non-reinforced failed (cracked) elbow specimens were repaired with CFRP wrapping. This part of the investigation is aimed at examining whether a cracked elbow, appropriately repaired, can fulfill its transportation function, resisting cyclic pressure and burst. Towards that purpose, a series of cyclic pressure and burst tests were performed.

First, the cracked specimens, with the exception of specimen 3, were sandblasted to clean the pipe surface. Then a GFRP (biaxial E-glass fabric with a weight of 813 g/m^2) patch was applied locally on the crack location to ensure water tightness, and subsequently, the elbows were wrapped with the same CFRP with the same procedure described in section 2.1 (Fig. 11). Table 3 presents the number of CFRP layers for each repaired specimen. The repaired specimens were subjected initially to constant pressure in order to examine water tightness, and subsequently, cyclic pressure was applied with a range from 5 to 50 bar by reaching an operational load level up to 33% Py for 1500 cycles. If the specimen resisted these 1500 pressure cycles, then the pressure was increased monotonically to burst.

Two specimens, namely 1 and 3, failed very early, at the first pressure cycle, before reaching the max pressure of 50 bar. Failure of specimen 1 was attributed to the fact that only one layer of CFRP had been used, which proved to be inadequate to achieve water tightness, even under rather low level of pressure. Failure of specimen 3 is probably attributed to the lack of any surface

preparation (sandblasting in this case), which ensures a high quality level of bonding between the composite and the steel. The other, two elbow specimens, namely 2 and 4 resisted the imposed 1500 pressure cycles, which means that their repair was successful. They were subsequently subjected to internal pressure up to burst and they failed, at pressures equal to 253 bar and 142 bar, respectively (Fig. 12).

These results are promising for the use of CFRP wrapping in repairing cracked piping components. However, further experiments are required to obtain better understanding of the effect of CFRP repairs on elbow performance against pressure.

Fig. 11: Repair of cracked non-reinforced specimens, with CFRP/GFRP wrapping.

Fig. 12: Burst and loss of containment in CFRP repaired specimens due to burst (specimen 4).

Table 3: Number of layers of CFRP patch reinforcement

Specimens	1	2	3	4
Number of layers	1	3	5	5

3 NUMERICAL MODELING

3.1 Finite element modeling description

A three-dimensional model was developed in general-purpose finite element program ABAQUS/Standard for simulating the experimental procedure. Elbow specimens, including the attached straight pipes, modeled using four-node, reduced-integration shell finite elements, denoted as S4R. The elbow diameter in the model was equal to 114.3 mm and the thickness was equal to 3.6 mm as shown in Fig. 13, while the boundary constraints at the upper and lower end of the pipe elbow specimen are presented in the Table 4.

In order to describe accurately the stress-strain response of steel material, material characterization tests were conducted on coupons extracted from the elbows both in monotonic and cyclic loading. An appropriate material model had also been adopted, to be presented in section 3.2, and inserted in the finite element model, as a user-defined material subroutine (UMAT) that accounts for the zero stress normal to the shell surface. This model has been introduced elsewhere [22], and has been shown to be very effective for the description of steel material behavior under severe cyclic plastic loading conditions.

The CFRP wrap (patch) was simulated as an additional layer of elastic shell elements with variable thickness; around the pipe, as shown in Fig. 14 (a). Because of pipe elbow geometry, wrapping of the CFRP material around the elbow results in different thickness of the CFRP wrap around the circumference (intrados versus extrados), due to the different level of overlapping. In order to simulate the variation of CFRP thickness, the model was partitioned into eight different areas around the circumference and, for each partition, a specific thickness was assigned based on thickness measurements on the actual CFRP patch, as shown in Fig. 14 (b). The analysis consists of two steps; in the first step, internal pressure was raised up to 4 bar, and in the second step, keeping the internal pressure constant, cyclic end displacement ΔL was applied, on the top hinge, as shown in Fig. 13.

Table 4: Boundary constraints.

R/M	Rx	Ry	Rz	Mx	My	Mz
RP1	Fixed	Fixed	ΔL	Free	Fixed	Fixed
RP2	Fixed	Fixed	Fixed	Free	Fixed	Fixed

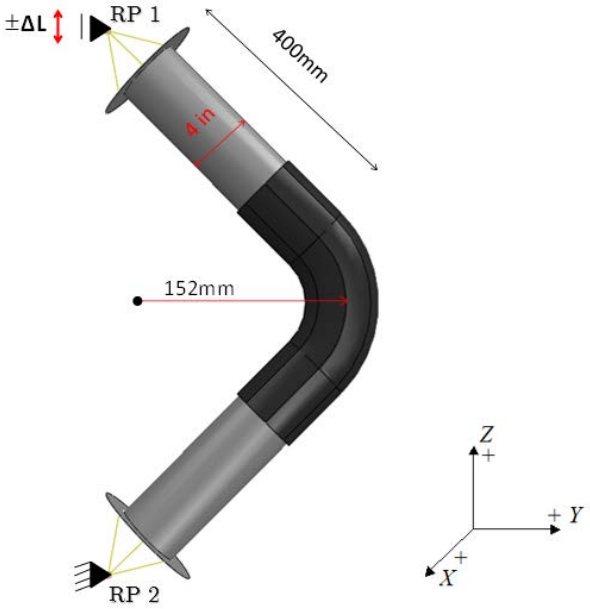

Fig. 13: Model of a reinforced pipe elbow with CFRP patch.

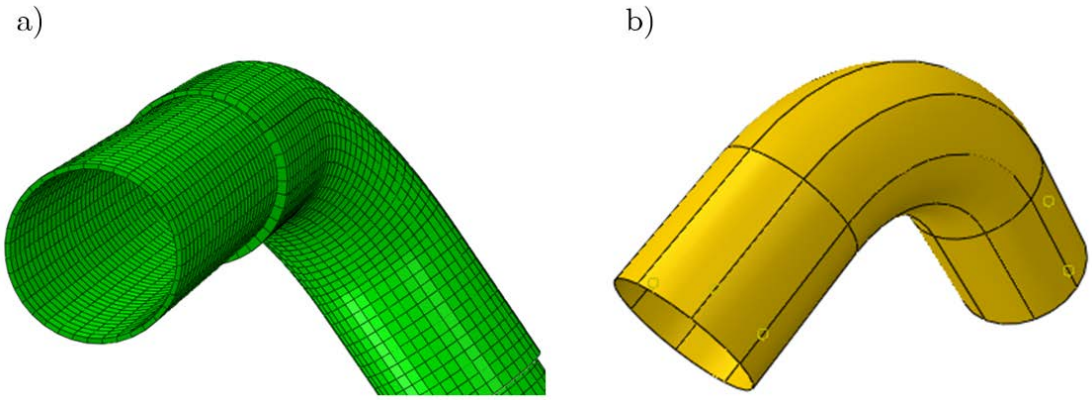

Fig. 14: a) Finite element model of reinforced pipe elbow with the CFRP patch; b) Partition of CFRP patch in eight sectors.

3.2 Constitutive modeling

The simulation of material behavior under reverse (cyclic) loading conditions is of major importance for modeling the structural capacity of elbows in a reliable manner. During cyclic loading, steel material behavior is characterized by two main features: (a) the plateau of the stress-strain curve in the first loading cycle (initial yielding), (b) the Bauschinger effect under reverse plastic loading, for the steel material under consideration; both features need to be accounted for the constitutive model. The model considered in the present study follows the nonlinear kinematic hardening rule, has been introduced elsewhere [22], and it is briefly described herein for the sake of completeness. The model adopts the von Mises yield surface given as follows:

$$F = \frac{1}{2}(\mathbf{s}-\mathbf{a})\cdot(\mathbf{s}-\mathbf{a}) - \frac{k^2}{3} = 0 \qquad (1)$$

where $\mathbf{s}$ is the deviatoric stress tensor, $\mathbf{a}$ is the "back stress" tensor and k is the size of the yield surface, which is a function of the value of the equivalent plastic strain ε_q, so that one may write $k = k(\varepsilon_q)$. The nonlinear kinematic hardening rule describing the evolution of back stress tensor is given by the following expression:

$$\dot{\mathbf{a}} = C\dot{\boldsymbol{\varepsilon}}^p - \gamma\mathbf{a}\dot{\varepsilon}_q \qquad (2)$$

where C, γ are nonlinear kinematic hardening parameters, calibrated from appropriate material testing results. The material model has been implemented through a user material subroutine (UMAT) in ABAQUS/Standard, using a robust "elastic predictor – plastic corrector" Euler-backward numerical integration scheme. More details of the proposed material model are provided in [22].

The model is calibrated using monotonic and cyclic tests of the steel material. Strip specimens were extracted from elbows in the longitudinal and hoop direction as shown in Fig. 15. More specifically, low-cycle fatigue (LCF) specimens were subjected to strain control cyclic tests, while tensile specimens were subjected to monotonic tests. From these tests, the average value of the yield stress is equal to $\sigma_y = 276\,\text{MPa}$, while the ultimate stress is equal to $\sigma_u = 467\,\text{MPa}$. Both

monotonic and cyclic experiments were conducted to the point of break. In Fig. 16 and Fig. 17 the stress-strain curves for monotonic and cyclic loading are shown respectively.

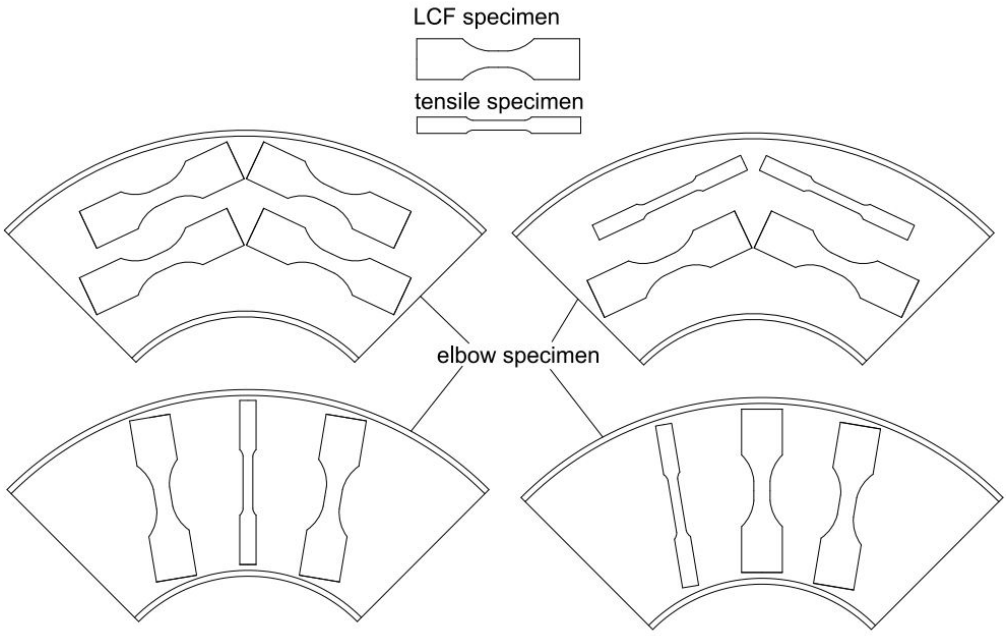

Fig. 15: Location of strip specimens extracted from the elbows.

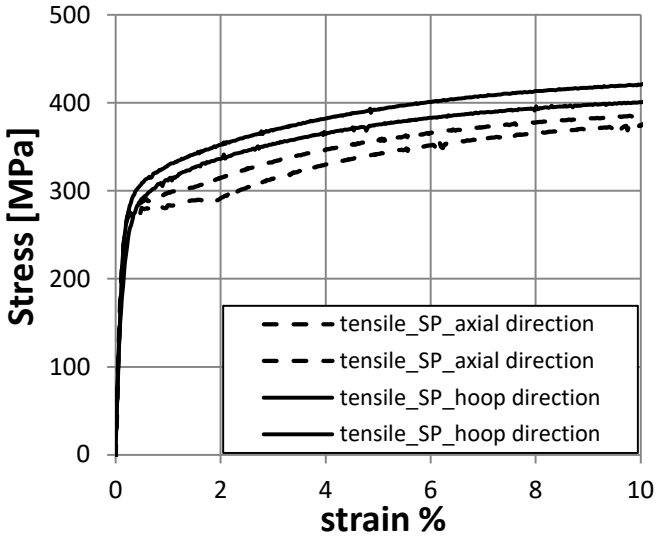

Fig. 16: Stress-strain curve from monotonic tests of P235 elbow material.

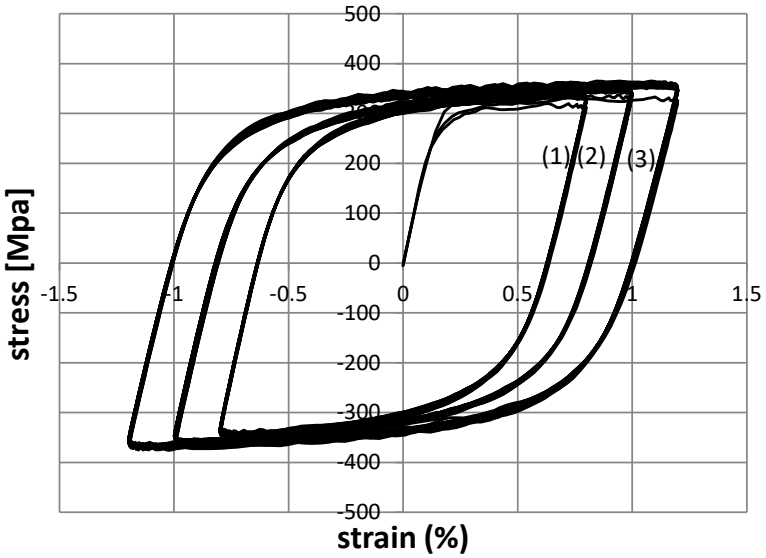

Fig. 17: Stress-strain curve of cyclic tests of P235 steel elbows material; strain ranges are: (1) $\pm 0.8\%$; (2) $\pm 1.0\%$; (3) $\pm 1.2\%$.

4 MECHANICAL BEHAVIOR OF PIPE ELBOWS SUBJECTED TO CYCLIC LOADING

4.1 Comparison between numerical and experimental results

A comparison between experiments and numerical results are presented in Fig. 18 and Fig. 19 in terms of force-displacement diagrams, for non-reinforced and for reinforced pipe elbows respectively. In the case of non-reinforced elbows, there is a good agreement in the load-displacement loops between the experimental and the numerical results. However, for the case of reinforced elbows, there is a certain difference in the load-displacement loops between experimental and the numerical results. This is attributed to the assumptions of the analysis on the modeling of CFRP wrapping. More specifically, the interaction between the pipe surface and the CFRP patch was assumed as a perfect bond. However, experimental observations (Fig. 7) indicate a degree of de-bonding between the steel pipe elbow and the CFRP wrap. Furthermore, the experimental results on the reinforced pipe elbows had shown a "special feature" on the load-displacement curve, in the form of a local peak of the load during the first loading cycle. This "first cycle peak" was apparent in the first cycle of all three tests, but disappeared in the subsequent cycles, and it was attributed to the cracks which occurred in the CFRP wrapping

during the first cycle. In subsequent cycles, no more cracks open in the CFRP material and, therefore, the load-displacement loop stabilizes.

In order to achieve a more realistic simulation, it should be useful to add an adhesive layer between the CFRP and the steel pipe elbow, considering appropriate cohesive properties so that the epoxy resin interface should be simulated more accurately. Furthermore, the cracks in CFRP fibers were not taken into account in our CFRP material model, and introduction of a local failure criterion and a progressive damage model would simulate CFRP behavior more realistically. Nevertheless, both the above possible amendments are outside the scope of the present study.

Fig. 20 to Fig. 22 depict a comparison between numerical and experimental results on the evolution of local strains at the flank location of the non-reinforced elbows. The comparison is quite satisfactory in terms of the range of hoop strain, whereas a fairly good agreement is found on the rate of strain evolution, often referred to as "ratcheting rate". Hoop strains from the experimental and numerical results indicate a maximum strain range from 1.5% to 2.5% for different values of applied displacement. Increasing the applied displacement range ΔL, the corresponding local strain range also increases, so that fatigue life decreases.

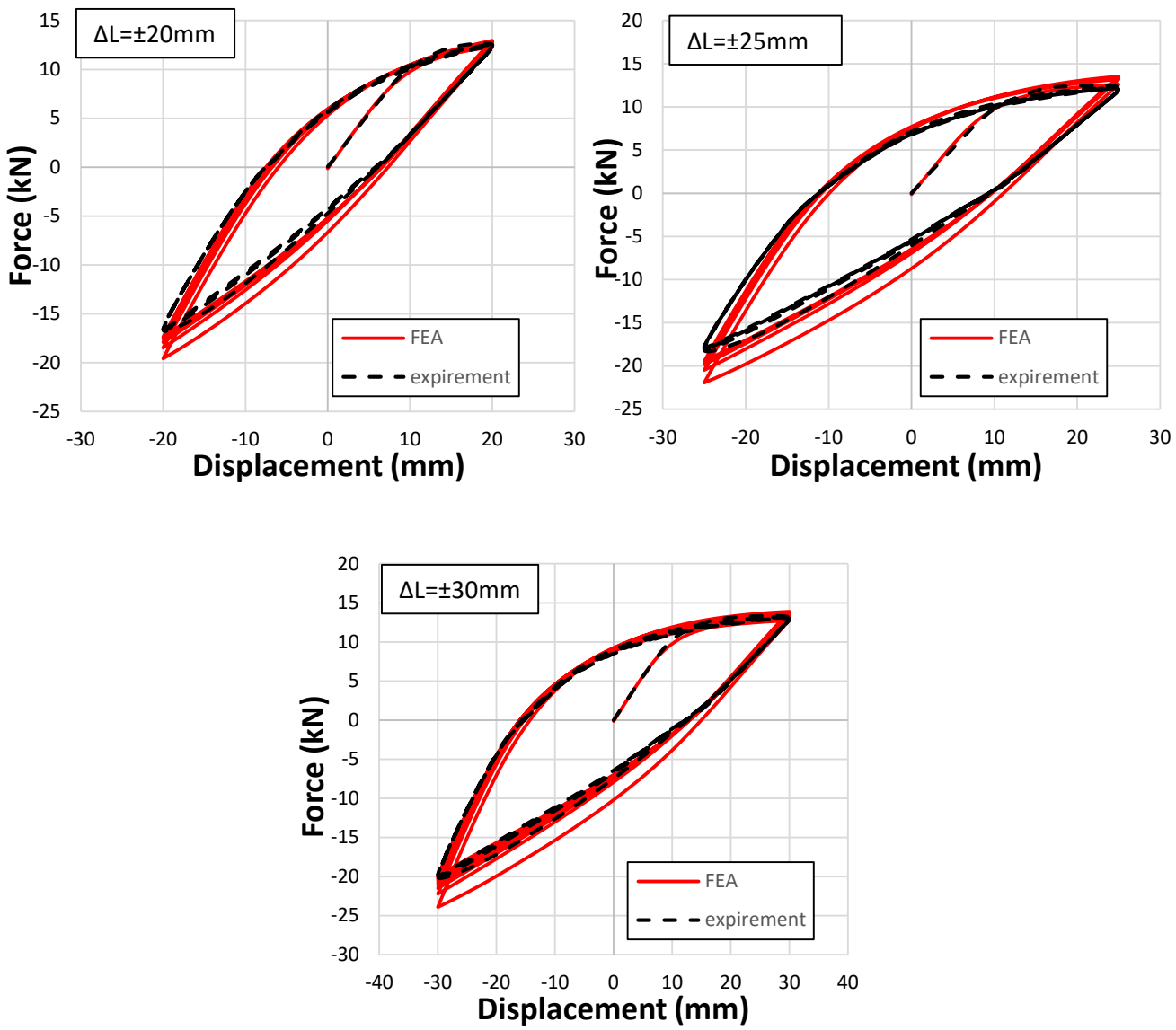

Fig. 18: Force (kN) versus displacement (mm) for ΔL equal to $\pm$20mm, $\pm$25mm, and $\pm$30mm; non-reinforced elbow specimens.

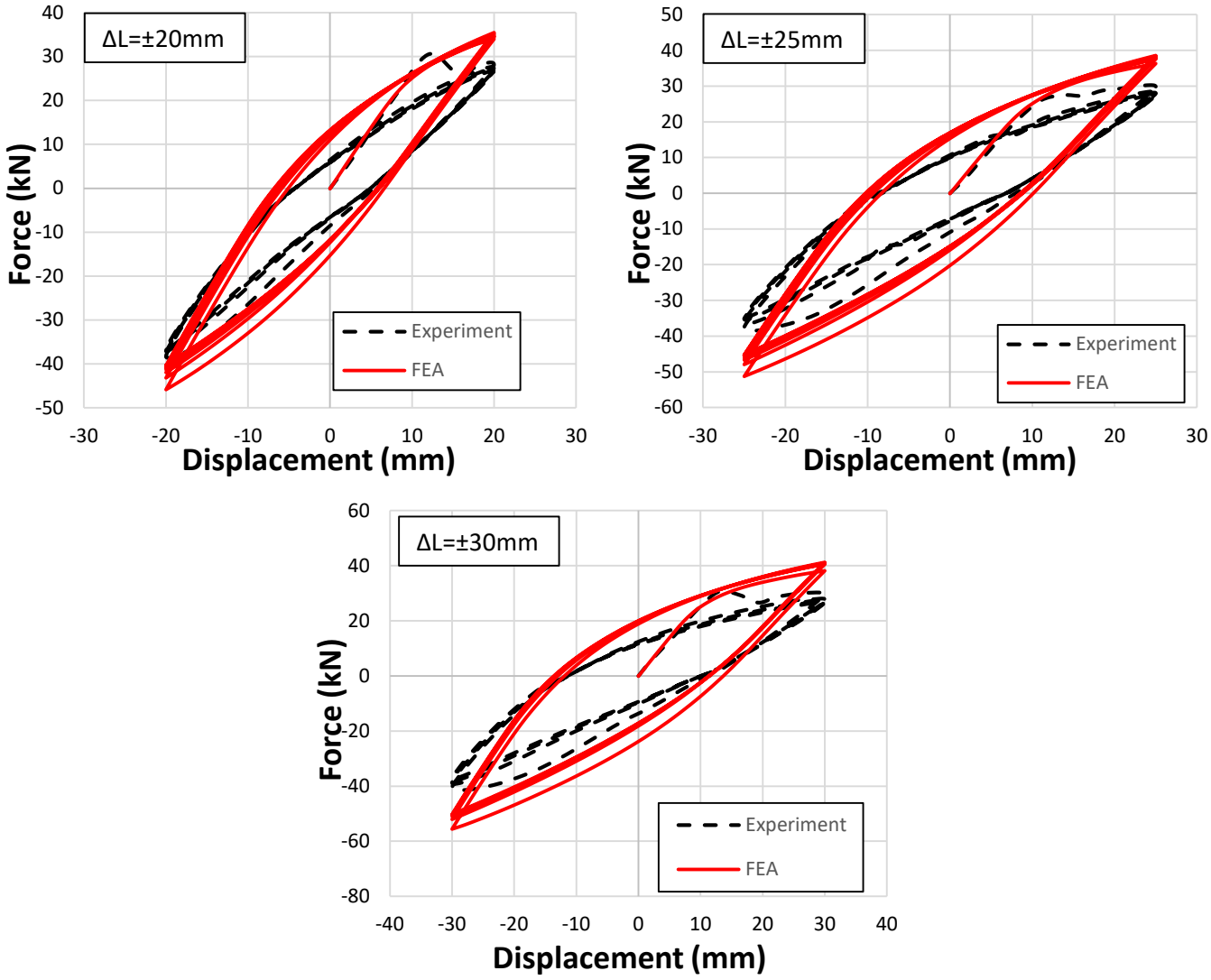

Fig. 19: Force (kN) versus displacement (mm) for ΔL equal to $\pm$20mm, $\pm$25mm, and $\pm$30mm; reinforced elbow specimens.

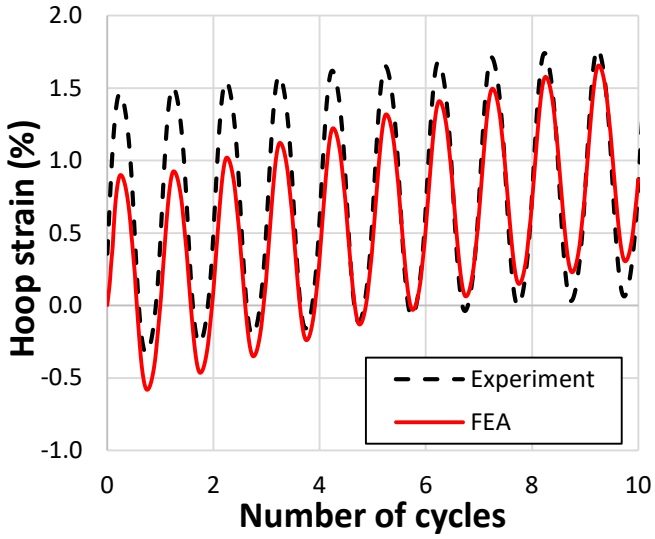

Fig. 20: Hoop strain evolution for ΔL equal to $\pm$20mm; non-reinforced elbow specimens.

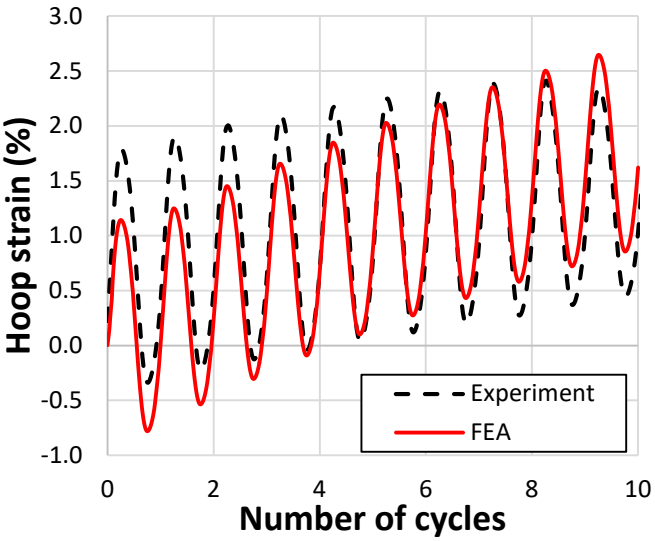

Fig. 21: Hoop strain evolution for ΔL equal $\pm$25mm; non-reinforced elbow specimens.

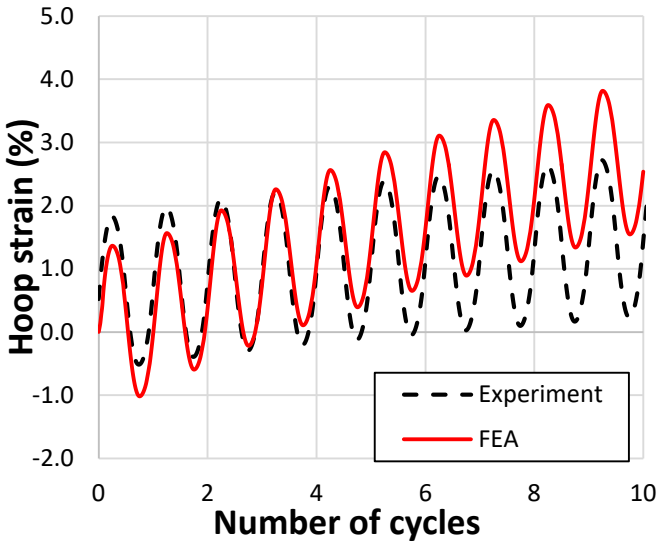

Fig. 22: Hoop strain evolution for ΔL equal $\pm$30mm; non-reinforced elbow specimens.

4.2 Comparison of reinforced and non-reinforced elbow behavior

In this section, a comparison of the structural response of reinforced and non-reinforced elbows subjected to cyclic loading with stroke ΔL equal $\pm$30mm is presented, in terms of local strains calculated from the numerical models at the critical location of each case. For the case of non-reinforced elbows, the maximum hoop strain is located at the elbow flank (crown), while in the reinforced elbow it is located at the elbow intrados. The results in Fig. 23 show that the maximum hoop strain developed in flank area for the case of non-reinforced elbow, is quite higher than the maximum hoop strain of reinforced elbow, which was developed in extrados surface. This is a direct consequence of the reduction of cross-sectional ovalization due to the presence of CFRP reinforcement as shown in Fig. 24. On the other hand, Fig. 25 shows that the maximum axial strain developed in the reinforced elbows in girth welds are higher than the maximum axial strains in non-reinforced elbows, which was developed in intrados surface. Furthermore, Fig. 23 and Fig. 25 show that the maximum strain in the case of non-reinforced elbow is mainly in the hoop direction, while in the case of reinforced elbow, the maximum strain is in the axial direction.

The distribution of strains in the case of applied displacement ΔL equal to $\pm$30mm is shown for the non-reinforced and the reinforced elbow in Fig. 26 and Fig. 27, respectively. Fig. 26 (a) and (b) show the distribution of hoop and axial strains at the outer surface of the non-reinforced elbow; in this case, hoop strains are always higher than the corresponding axial strains. Finally,

Fig. 26 (c) presents the distribution of equivalent plastic strain in the non-reinforced elbow; the regions with significant plastic deformation are located mainly at elbow crown (flank), an observation which is in accordance with the location and direction of the crack observed experimentally (Fig. 4).

Fig. 27 (a) and (b) show the distribution of hoop and axial strains respectively at the outer steel surface of the reinforced elbow. The main observation is that, in reinforced elbows, axial strains are higher than the corresponding hoop strains. Fig. 27 (c) depicts the distribution of equivalent plastic strain, which differs substantially from the corresponding distribution in the non-reinforced elbow, shown in Fig. 26 (c). The fact that the axial strains are more significant than hoop strains in reinforced elbows is also in agreement with the experimental results; fatigue cracks occurred at the girth weld of the elbow with the straight parts, directed in the hoop direction of the pipe (Fig. 6), due to the development of excessive axial strains.

Furthermore, considering the equivalent plastic strain as a measure of accumulation of fatigue damage, the numerical results show that the level of equivalent plastic strain developed in reinforced elbows is lower than in the non-reinforced elbows, so the fatigue life of reinforced elbows is expected to be higher than the fatigue life of the non-reinforced elbows, which is also in good agreement with experimental results.

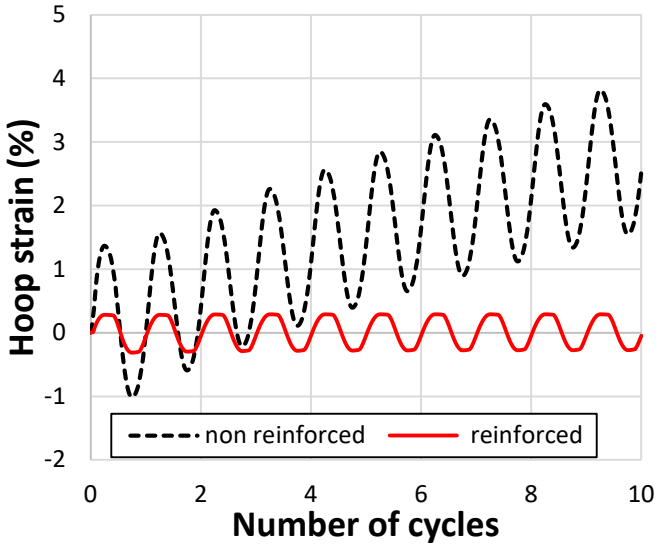

Fig. 23: Hoop strain evolution for ΔL equal to $\pm$30mm; non-reinforced and reinforced elbows.

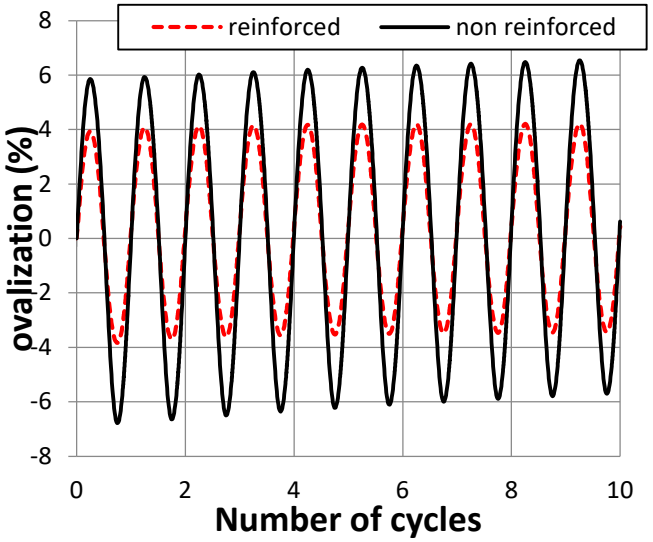

Fig. 24: Evolution of ovalization in non-reinforced and reinforced elbows for ΔL equal to $\pm$30mm.

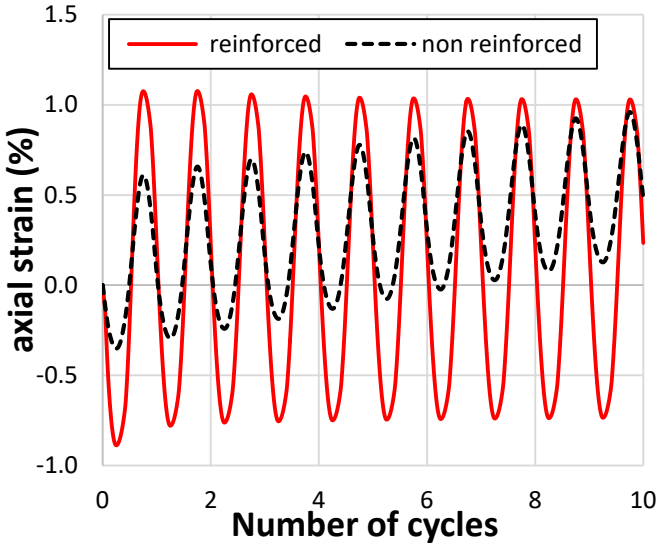

Fig. 25: Axial strain evolution in non-reinforced and reinforced elbows for ΔL equal to $\pm$30mm.

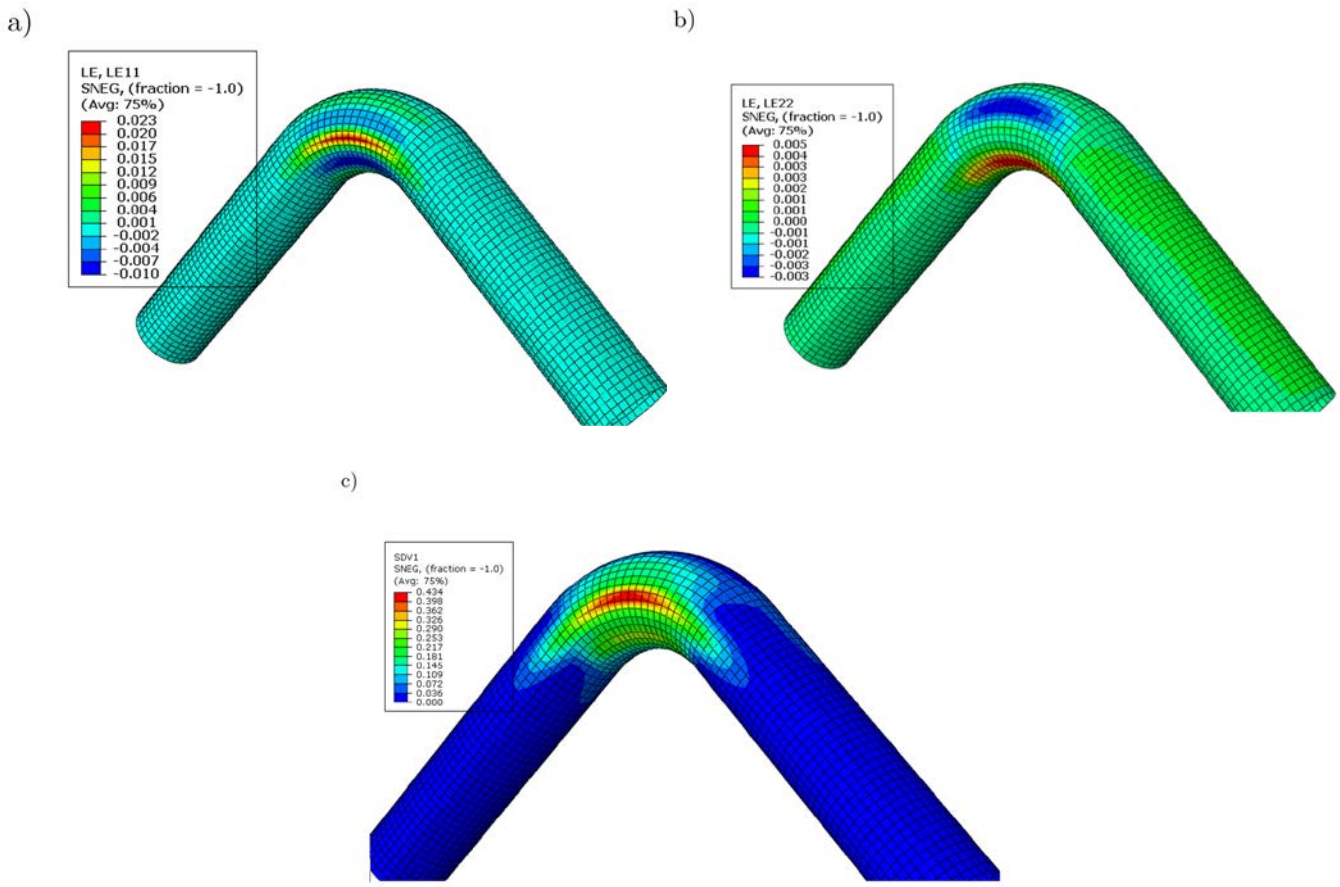

Fig. 26: Distribution of strains in non-reinforced elbows for ΔL equal to $\pm$30mm; (a) hoop strains; (b) axial strains; (c) equivalent plastic strains.

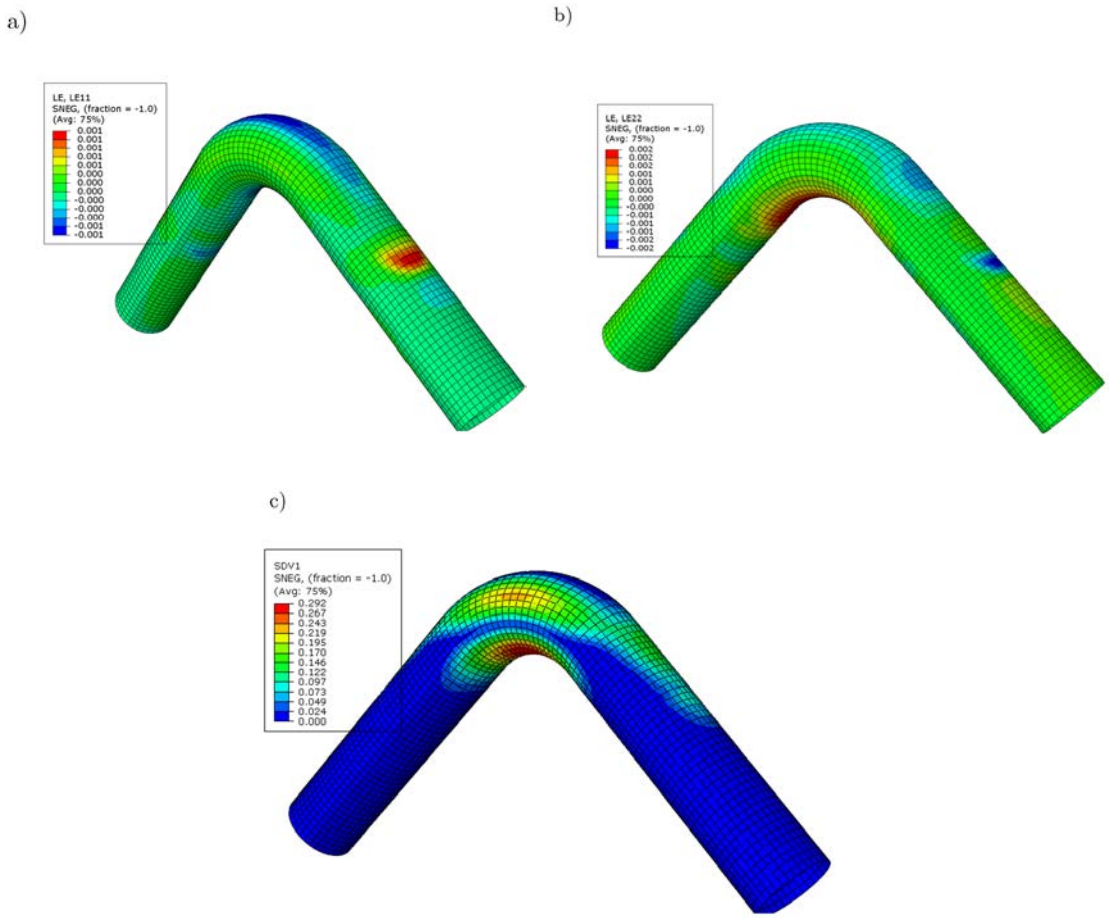

Fig. 27: Distribution of strains in reinforced elbows for ΔL equal to ±30mm; (a) hoop strains; (b) axial strains; (c) equivalent plastic strains.

4.3 Effect of internal pressure

The effect of internal pressure on the structural response of the elbows under consideration, subjected to repeated loading is examined in this paragraph using the numerical tools described previously. In particular, the case of applied displacement ΔL equal to ±25mm is considered, at four levels of internal pressure, as a percent of the nominal yield pressure of the pipe cross-section ($p_Y = 2\sigma_Y t/D$), which is equal to 17.38 MPa.

The numerical results for non-reinforced elbows (Fig. 28) indicate that, as internal pressure increases, the elbow becomes somewhat stiffer, exhibiting a "cyclic stiffening effect". Furthermore, the maximum value of hoop strain, observed in the flank area, increases with respect to the non-pressurized case, due to biaxial ratcheting (Fig. 29), despite the fact that

cross-sectional ovalization is less pronounced. On the other hand, results on reinforced elbows shows that the presence of internal pressure may not have a significant influence on structural response (Fig. 30). In particular, there exists a small effect of internal pressure on local strains for the reinforced elbows. Furthermore, in this case no ratcheting effect is detected, as shown in Fig. 31 and Fig. 32 and this implies that the effect of pressure on the response of cyclic loaded CFRP reinforced elbows might not be very important in terms of their fatigue life. Nevertheless, an experimental verification could be useful in order to investigate more precisely the effect of pressure on the fatigue life of reinforced elbows. Such an experimental study is outside the scope of the present study.

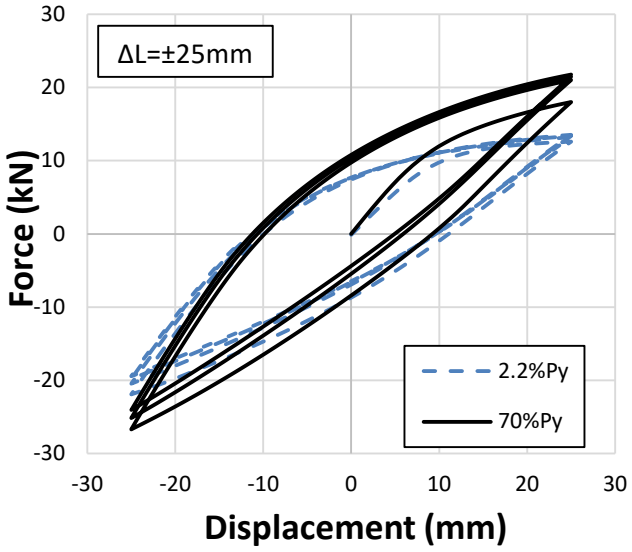

Fig. 28: Force (kN) versus displacement (mm) for ΔL equal to ±25mm for different levels of internal pressure; non-reinforced elbow specimen.

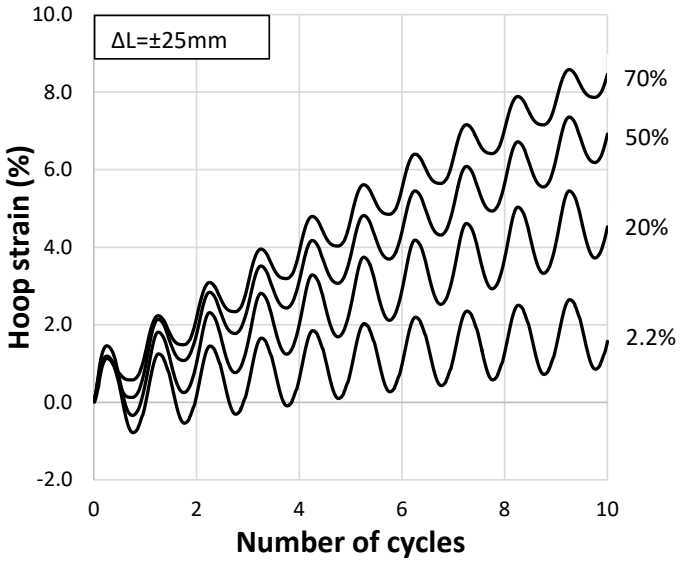

Fig. 29: Hoop strain evolution for ΔL equal to ±25mm for different levels of internal pressure as a percent (%) of yield pressure; non-reinforced elbow specimen.

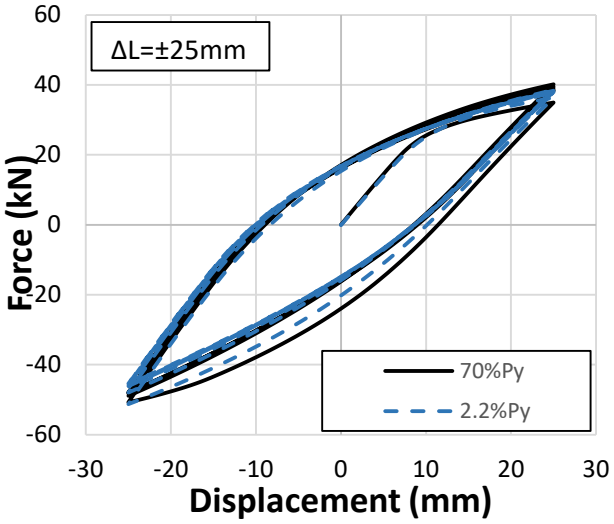

Fig. 30: Force (kN) versus displacement (mm) for ΔL=±25mm for different levels of internal pressure; reinforced elbow specimen.

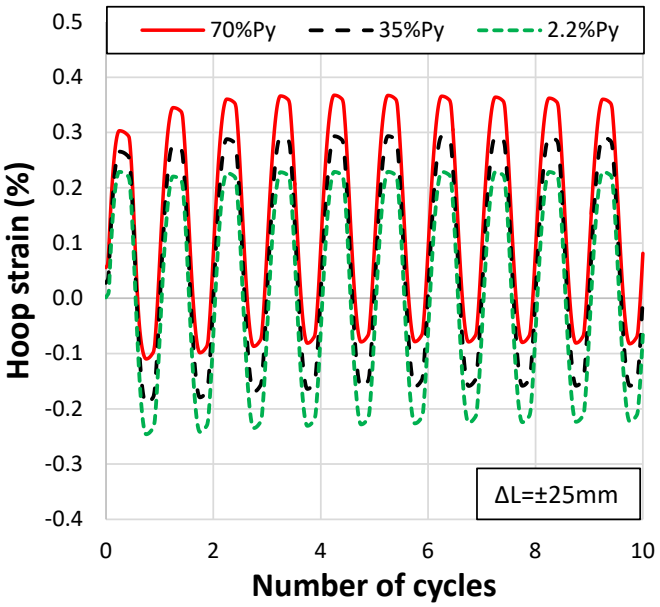

Fig. 31: Hoop strain evolution for ΔL equal to ±25mm for different levels of internal pressure; reinforced elbow specimens.

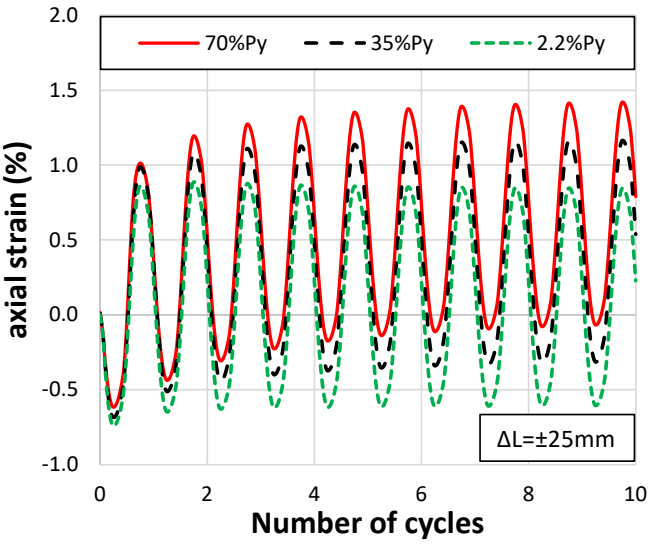

Fig. 32: Axial strain evolution for ΔL equal to ±25mm for different levels of internal pressure; reinforced elbow specimens

5 CONCLUSIONS

The mechanical performance for non-reinforced and CFRP-reinforced pipe elbows under severe cyclic loading conditions has been studied experimentally, and supported by numerical simulations. Various ranges of constant amplitude end-displacement were applied, leading to low-cycle fatigue. The results show that the CFRP patch increases the corresponding reaction force almost 2.5 times, for all displacement ranges studied. Furthermore, a significant increase of loading cycles until failure has been observed in the experiments: for an applied displacement range of ±20mm, the reinforced elbow is capable of sustaining a number of loading cycles almost 3.5 times higher than the non-reinforced elbow, whereas for applied displacement ranges equal to ±25mm and ±30mm, the fatigue life has been improved by a factor 2.6 and 2 respectively. The main result has been that the CFRP reinforcement reduces cross sectional ovalization, resulting in lower strains within the elbow. Moreover, the numerical results have clearly indicated that strains in hoop direction were significantly lower in the case of reinforced than non-reinforced pipe elbow. Because of these lower values of strains, the fatigue life of the reinforced pipe elbow increases. Furthermore, pressure tests on cracked elbow specimens have demonstrated that sandblast and an adequate number of CFRP layers are required in order to repair successfully pipe elbows using composite materials, towards their safe operation.

The basic conclusion from this work is that appropriate reinforcement of steel pipe elbows with CFRP wrap material constitutes a promising method for simple and efficient improvement of their mechanical behavior and integrity under severe structural loading, increasing their ultimate strength and their fatigue life against low-cycle fatigue cracking.

ACKNOWLEDGEMENT

The authors would like to thank FYFE Europe S.A. for providing the CFRP wrapping for the pipe elbows, tested in the present study.

REFERENCES

[1] Sobel, L. H and Newman, S. Z., "Comparison of Experimental and Simplified Analytical Results for the In-Plane Bending and Buckling of an Elbow", *ASME J. Pressure Vessel Technology*, Vol. 102, pp. 400-409, 1980.

[2] Peters, F E.,, "Results from a Buckling Test of a 16-Inch (406 mm) Diameter Piping Elbow", *Westinghouse Advanced Reactors Division Topical Report*, WARD-HT-3045-35, 1978.

[3] Gresnigt, A. M., Van Foeken, R., "Strength and Deformation Capacity of Bends in Pipelines", *Int. Journal of Offshore & Polar Eng.*, Vol. 5, pp. 294-307, 1995.

[4] Chattopadhyay J., Nathani, D.K., Dutta, B.K., Kushwaha, "Closed-Form Collapse Moment Equations of Elbows Under Combined Internal Pressure and In-Plane Bending Moment", *ASME PPVP Conference, Seismic engineering*, Vol 137, 2000.

[5] Yahiaoui, K., Moffat, D. G., and Moreton, D. N., "Response and Cyclic Strain Accumulation of Pressurized Piping Elbows under Dynamic in-Plane Bending", *J. Strain Analysis in Engineering Design*, Vol 31, pp. 135-151, 1996.

[6] Fujiwaka, T., Endou, R., Furukawa, S., Ono, S., Oketani, K., "Study on Strength of Piping Components Under Elastic-Plastic Behavior Due to Seismic Loading", *ASME PVP Conference, Seismic engineering*, Vol 137., 1999.

[7] Karamanos, S. A., Giakoumatos , E., Gresnigt, A. M, "Nonlinear Response and Failure of Steel Elbows Under In-Plane Bending and Pressure", *ASME Journal of Pressure Vessel Technology,* Vol 125, pp. 393-402, 2003.

[8] Karamanos, S. A., Tsouvalas, D., Gresnigt, A. M., "Ultimate Bending Capacity and Buckling of Pressurized 90 deg Steel Elbows", *ASME Journal of Pressure Vessel Technology*, Vol. 128, pp.135-151, 2006.

[9] Pappa, P., Tsouvalas, D., Karamanos, S. A., and Houliara, S., "Bending Behavior of Pressurized Induction Bends", *Offshore Mechanics and Arctic Engineering Conference, Lisbon*, Portugal, 2008.

[10] Takahashi, K., Tsunoi, S., Hara, T., Ueno, T., Mikami, A., Takada, H., Ando, K., Shiratori, M., "Experimental study of low cycle fatigue of pipe elbows with local wal thinning and life estimation using finite element analysis", *International Journal of Pressure Vessels and Piping*, Vol 87, pp. 211-219, 2009.

[11] Varelis, G. E., Karamanos, S. A., Gresnigt, A. M, "Pipe Elbows Under Strong Cyclic Loading", ASME Journal of Pressure Vessel Technology, Vol 135. Paper No.011207, 2013.

[12] Varelis, G. E., and Karamanos, S. A.. "Low-Cycle Fatigue of Pressurized Steel Elbows Under In-Plane Bending", *Journal of Pressure Vessel Technology*, Vol 137, No. 011401, 2015.

[13] Karamanos S. A, "Mechanical Behavior of Steel Pipe bends: An Overview", *Journal of Pressure Vessel Technology,* Vol. 138(4), 2016.

[14] Alexander, C.R, "Assesing the Use of Composite Materials in Repairing Mechanical Damage in Transmission Pipelines", *Proceeding of the 6th International Pipeline Conference*, Calgary, Alberta, Canada, 2006.

[15] Alexander, C. R, "Recent Advances on the Evaluating Composite Repair Technology Used to Repair Transmission Pipelines", *Clarion Evaluation and Rehabilitation of Pipelines Conference*, 2009.

[16] Alexander, C., Bedoya, J., "Repair Of Dents To Cyclic Pressure Service Using Composite Materials", *Proceeding of the 8th International Pipeline Conference*, Calgary, Alberta, Canada, 2010.

[17] Alexander, C., Kania, R., Zhou, J., Vyvial, B., Iver, A., "Reinforcing Large Diameter Elbows Using Composite Materials Subjected To Extreme Bending and Internal Pressure Loading", *Proceeding of the 11th International Pipeline Conference*, Calgary, Alberta, Canada, 2016.

[18] Chan, P. H., Tshai, K. Y., Johnson, M., Li, S., "Finite Element Analysis of Combined Static Loadings on Offshore Pipe Riser Repaired with Fibre-Reinforced Composite Laminates", *Journal of Reinforced Plastics and Composites*, Vol. 33(6), pp.514-525, 2014.

[19] Mokhtari, M., Alavi Nia, A., "The influence of Using CFRP Wraps on Performance of Buried Steel Pipelines Under Permanent Ground Deformations", *Journal of Soil Dynamics and Earthquake Engineering*, Vol. 73, pp. 29-41, 2015.

[20] Mokhtari, M., Alavi Nia, A., "The Application of CFRP to Strengthen Buried Steel Pipelines Against Subsurface Explosion", *Journal of Soil Dynamics and Earthquake Engineering*, Vol. 87, pp. 52-62, 2016.

[21] Reich, A., Charest, J., "Carbon Fiber Reinforcement of a Water Storage Tank for Beyond Design Basic Loads", *Proceedings of Pressure Vessels and Piping Conference PVP2016*, Vancouver, Canada, 2016.

[22] Chatzopoulou, G., Karamanos, S. A., and Varelis, G. E., "Finite Element Analysis of UOE Manufacturing Process and its Effect on Mechanical Behavior of Offshore Pipes", *International J. Solids and Structures*, Vol. 83, pp. 13-27,2016.